Article

Assessment of soil erosion at multiple spatial scales following land use changes in 1980-2017 in the black soil region, (NE) China

Haiyan Fang [1,3] and Zemeng Fan [1,2,3]

[1] Key Laboratory of Water Cycle and Related Land Surface Processes, Institute of Geographic Sciences and Natural Resources Research, Chinese Academy of Sciences, Beijing 100101, China

[2] State Key Laboratory of Resources and Environmental Information System, Chinese Academy of Sciences, Beijing 100101, China

[3] College of Resources and Environment, University of Chinese Academy of Sciences, Beijing 100049, China

* Correspondence:Corresponding authors: fanghy@igsnrr.ac.cn, Tel/Tex: +86-010-64883172; fanzm@lreis.ac.cn, Tel/Tex: /+86-010-64889169

Abstract: Impact of land use and land cover (LULC) change on soil erosion is still imperfectly understood, especially in northeastern China (NEC). Based on the Revised Universal Loss Equation (RUSLE), the variability of soil erosion at different spatial scales following land use changes in1980, 1990, 2000, 2010, and 2017 was analyzed. The regionally spatial patterns of soil loss coincided with the topography, rainfall erosivity, soil erodibility, and use patterns, and around 45% soil loss came from arable land. Regionally, soil erosion rates increased from 1980 to 2010 and decreased from 2010 to 2017, ranging from 3.91 to 4.45 t ha^{-1} yr^{-1} with an average of 4.22 t ha^{-1} yr^{-1} in 1980-2017. The rates of soil erosion less than 1.41 t ha^{-1} yr^{-1} decreased from 1980 to 2010, and increased from 2010 to 2017, and opposite changing patterns occurred in higher erosion classes (i.e., above 5 t ha^{-1} yr^{-1}). At a provincial scale, Liaoning Province experienced the highest soil erosion rate of 9.43 t ha^{-1} yr^{-1}, followed by Jilin Province, the east Inner Mongolia, and Heilongjing Province. Arable land continuously increased at the expense of forest in the high-elevation and steep-slope areas from 1980 to 2010, and decreased from 2010 to 2017, resulting in increased areas with erosion rates higher than 7.05 t ha^{-1} yr^{-1}. At a county scale, around 75% of the countries had soil erosion rate higher than its tolerance level. The county numbers with higher erosion rate increased in 1980-2010 and decreased in 2010- 2017, resulting from the sprawl and withdrawal of arable land. The results indicate that appropriate policies can control soil loss through limiting arable land sprawl in areas of unfavorable regions in the NEC.

Keywords: Soil erosion; land cover change; RUSLE; the northeastern China

1. Introduction.

In recent decades, soil erosion induced by land use and land cover (LULC) change has become a hot issue [1]. The rapid expansion of arable land at the expense of natural vegetation induces environmental problems such as land degradation, river and reservoir sedimentation, and freshwater pollution [2]. A deep understanding of LULC-induced spatio-temporal patterns of soil erosion is of great importance to land use management.

Impact of LULC change on soil erosion has been done at multiple scales, from plot [3-4], catchment [5], regional [6], and to global scales [7]. Borrelli et al [7] concluded an overall increase in global soil erosion induced by cropland expansion, and 35.9 Pg yr^{-1} soil was eroded away from the earth surface. In Europe, soil loss from the agricultural land accounts for 93.5% of the total. At a catchment scale, studies concluded that in comparison to climate change, soil erosion is more sensitive to LULC change [8]. At a plot scale, more attention was focused on the impact of key

factors such rainfall intensity, vegetation type and coverage on soil loss. For example, Anh et al. [3] examined the impact of interactions of vegetation cover and soil macronutrient levels on soil erosion at 30 plots in a hilly area, northern Vietnam. Anache et al [4] found that soil loss from plots was affected by land use types and their combination patterns. Until today, more work has been done to quantify the impact of the changing LULC on soil erosion at an individual scale, whereas less attention was paid to identify their variations with varied spatial scales, following LULC changes.

The northeastern China (NEC) belongs to one of the three major black soil regions in the world, where the fertile soils have rich soil organic carbon and superior physical and chemical characteristics. The NEC is one of the most important grain production areas in China [9]. However, the soil depth has decreased from around 100 cm in its original cultivation period to 20-30 cm at current time [10], due to extensive expansion of arable land and increasing population pressure [11-12].

Since the end of the 20th century, the severe soil erosion has been recognized, and studies have been done in the NEC using runoff plots [13-14], tracers [15], and soil erosion models [10, 16]. The impacts of land use on soil erosion have also been done. For example, Ouyang et al. [17] examined the combined impacts of land use and soil property changes in 1979-2014 on soil erosion in a 142.5 km^2 Bawujiu Farm. Fang [18] examined the relative contributions of land use change and dam construction to sediment yield in the Shuangyang River catchment, NEC. At a large spatial scale, Jiang et al. [19] studied the impact of land use change in 2000-2010 on soil erosion in Heilongjiang Province. These studies improve our understanding of the impact of LULC change on soil erosion. However, a lack of reliable estimate of the entire NEC forces scientific community to resort to these pioneering studies. A deep insight of soil erosion characteristics for the entire NEC spanning the most recent years is thus urgently required.

Soil erosion modeling is an efficient method to explore LULC change impact on soil erosion and sediment yield [8]. Process-based models are complex and require substantial data, which usually preclude their broad application, especially in developing countries or remote regions. In contrast, a simple, physically plausible empirical model such as the Revised Universal Soil Loss Equation (RUSLE) is usually welcome, especially at regional and/or global scales [7].

Therefore, the RUSLE model was used in this study to (i) quantitatively evaluate the trend of soil erosion for the entire NEC from 1980 to 2017, (ii) explore the characteristics of spatio-temporal of soil erosion, and (iii) analyze the contribution of changing LULC to soil loss during the past decades.

2. Materials and methods

2.1. Study area

The NEC (38º42'-53º36', 115º24'-135º12') includes three provinces (i.e., Heilongjiang, Jilin, and Liaoning province) and the east Inner Mongolia Autonomous Region (IMA) (Figure 1a). It covers an area of 1.24 million km^2, with elevation ranging from -10 to 2666 m a.s.l. The NEC is composed of three mountains, three plains, and three large rivers. The Da Hinggang Mountain, the Xiao Hinggang Mountain, and the Changbai Mountain lie in the northwest, northeast, and southwest, respectively. Three plains including Liao River Plain, Songnen Plain, and Sanjiang Plain are situated between the mountains. They were formed by the piedmont alluvial and flood sedimentation from Heilong River, Songhua River, and Tumen River that join at the east of Sanjiang Plain. The slopes range from zero in the plains to above 60° in the mountainous regions (Figure 1b).

The NEC has a continental climate. The annual precipitation in 1970-2018 ranged from around 993 mm in the southeast to less than 242 mm in the northwest (Figure 1c), around 65% of which fell in summer (i.e., June-August). The temperature varies greatly, with the highest mean monthly temperature 18℃ in July, and the lowest temperature -20℃ in January.

Affected by the summer monsoon from the southeast and obstruction by the Chanbai Mountain, the vegetation in the NEC is distributed zonally, from forest to the east of the Changbai Mountain, to a transition zone between forest and grass lands in the Songnen Plain, and to grassland to the west of the Da Hinggang Mountain (Figure 1b). Coniferous forest is mainly distributed in the

mountainous areas, and broad leaved forest scatter in the plains. Arable land in the plains covers about one third of the total area. The main crops are maize, soybean, and rice, occupying around 87% of the total. A single tillage operation is typically used with a cultivation harrow with 0.25 m depth in late-September and in early-May. From October to April, arable land is left fallow with no vegetation cover during cold weather.

The main soil types are Luvisols, Phaeozems, Chernozems, and Gleysols, occupying 37.5%, 23.3%, 7.4%, 6.8% of the total area in the NEC (Figure 1d). The parent materials are Quaternary lacustrine and fluvial sand beds or loess sediments [20]. Fuvisols are widely distributed in mountainous areas, while Phaeozems and Chaeozems which are called black soils by local people mainly appear in the Songnen Plain [9]. The textural classes of the topsoil are silt-clay-loam to clay-loam (8-27% sand, 29-66% silt and 26-40% clay), with soil organic carbon usually above 4%. The hilly regions with long slope in the mountain-plain transition zone are prone to soil erosion. Rill erosion dominates the study area. However, gullies also widely occur [16].

Figure 1 is about here.

2.2. Data collection

The RUSLE (Revised Universal Soil Loss Equation) was employed to estimate soil erosion rate. Several data layers are required to run this model: a Digital Elevation Model (DEM), land use maps, a rainfall erosivity map, a soil erodibility map, the land use management and soil conservation practice maps.

The DEM was prepared from Shuttle Radar Topography Mission (SRTM) with 90-m resolution. It was provided by Geospatial Data Cloud site, Computer Network Information Center, Chinese Academy of Sciences (http://www.gscloud.cn).

The Harmonized World Soil Database (HWSD) Version 1.2 was obtained from Food and Agriculture Organization of the United Nations (FAO-UN; http://www.fao.org). Soil properties such as percentages of sand, clay and silt, depth of soil, organic carbon are available from the HWSD.

The daily precipitation data in 1970-2018 at the 120 meteorological stations were acquired from National Climate Centre of the China Meteorological Administration (http://data.cma.cn/).

The land use datasets with 30-m resolution were acquired from different sources. The datasets in 1980, 1990 and 2010 were obtained from the Resource and Environmental Sciences, Chinese Academy of Sciences (RES-CAS). The datasets in 2010 and 2017 were downloaded from the GlobeLand30 (http://www.globallandcover.com) and from the research team of Gong Peng in Tsinghua University (http://data.ess.tsinghua.edu.cn/fromglc2017v1.html).

2.3. Description of the RUSLE and data treatment

In the present study, soil erosion intensity was calculated using RUSLE. It combines five factors, including rainfall erosivity, soil erodibility, slope length and gradient, land use management, and soil conservation practices:

$$A = R * K * LS * C * P \qquad\qquad (1)$$

where A is the soil erosion rate (t ha^{-1} yr^{-1}), R is the rainfall-runoff erosivity factor (MJ mm ha^{-1} h^{-1}), K is the soil erodibility factor (t ha h ha^{-1} MJ^{-1} mm^{-1}), LS is a combination of slope length L and slope gradient S factor (-), C is the crop/cover management factor (-), and P is the soil conservation factor (-).

The classic method to calculate R factor is to multiply rainfall energy and the maximum 30-min rainfall intensity for rainfall events [21]. However, such datasets are not available for many places in the world. In such instances, alternative method has been proposed to calculate *R* factor using readily available precipitation data [22-23]. In the current study, the daily precipitation data in 1970-2018 was used to estimate mean annual R-factor values, using the method proposed by Zhang et al. [23]:

$$R_i = a\sum_{j=1}^{k}(D_j)^b \qquad (2)$$

Where R_i is the half-month R-factor (MJ mm ha^{-1} h^{-1} yr^{-1}), and D_j is the erosive rainfall day j. D_j is equal to actual rainfall when it is greater than 12 mm. Otherwise it equal to zero. Here, *a* and *b* are empirical parameters. Detailed description was given by Fang and Sun (2017). A Co-Kriging interpolation was used to derive an R-factor value map in ArcGIS 10.5 software. In the NEC, mean annual R-factor values ranged from 475 in western NEC to 5320 MJ mm ha^{-1} h^{-1} yr^{-1} in southeastern NEC (Figure 2a).

Figure 2 is about here.

Soil texture and soil organic matter of the top 30 cm soils were available from the HWSD, and the K factor values were calculated by using EPIC method. This method has been successfully used in the NEC[10,17]:

$$K = 0.2 + 0.3e^{[-0.0256SAN(1-SIL/100)]} * (\frac{SIL}{CLA+SUK})^{0.3} * \left[1 - \frac{0.25SC}{SC + e^{(3.72-2.95SC)}}\right]$$
$$* \left[1 - \frac{0.72SN}{SN + e^{(22.9SN-5.51)}}\right] \qquad (3)$$

where *SAN* is the sand content (%), *SIL* is the silt content (%), *CLA* is the clay content (%), *SC* is the soil organic carbon content (%) and *SN* = 1-*SAN*/100. The K factor values of the study region varying from 0 to 0.045 t ha^{-1} h MJ^{-1} mm^{-1} ha^{-1} (Figure 2b).

The L-factor measures the slope length, and S-factor is proportional to the local slope. This study used the 2D approach to calculate LS factor as proposed by Van Rompaey et al.[24], using the methods by McCool et al.[25] and Desmet and Govers[26]:

$$L_{ij} = \frac{(A_{i,j}+D^2)^{m+1} - A_{i,j}^{m+1}}{D^{m+2}*x_{i,j}^{m}*22.13^{m}} \qquad (4)$$

$$x_{i,j} = sin\alpha_{i,j} + cos\alpha_{i,j} \qquad (5)$$

$$m = \frac{\beta}{(1+\beta)} \qquad (6)$$

$$\beta = \frac{(sin\theta/0.0896)}{[3*(sin\theta)^{0.8}+0.56]} \qquad (7)$$

$$S = \begin{cases} 10.8sin\theta + 0.03, \theta < 9\% \\ 16.8sin\theta - 0.5, \theta \geq 9\% \end{cases} \qquad (8)$$

where $L_{i,j}$ is the slope length factor of the grid cell with coordinates i and j, $A_{i,j}$ is the contribution area at the inlet of a pixel (m^2), D is the grid cell size (m); $\alpha_{i,j}$ is the slope aspect direction for a pixel; m is slope length exponent, β is empirical factor (-), and θ is the slope angle. The derived LS factor values ranged from 0.03 to 70.02. Higher values occurred in the mountainous regions, and lower values in the plains (Figure 2c).

The *C* and *P* factors closely link to land use types [27]. In order to obtain reasonable C- and P-factor values, a detailed survey of the literatures published in the NEC was first carried out [19, 28-31]. Then, C-factor values in forest, grassland, shrub land, cultivated land, and residential area were assigned to 0.004, 0.043, 0.07, 0.228, 0.03, and those in bare land, wetland and water bodies, and other unused land were 1, 0, and 0.06, respectively. For P-factor values, cultivated land and water body were set to 0.352 and 0, and other lands were unit in the study area.

3. Results

3.1. LULC changes in the NEC

The land uses in 1980-2017 were shown in Figure 3 and numerically in Table 1. Spatially, forests were distributed in mountainous areas, and arable lands in the three plains. Among the land use

classes, forest was predominant and covered 37% of the whole area, followed by arable- and grass-land covering 30% and 22%, respectively. These three kinds of lands occupied around 90% of the total. Shrub land, wetland, water body, and unused lands each covered 2% of the total area.

Table 1 is about here.

Figure 3 is about here.

During the past decades, great changes in arable land and forest occurred. Before 2010, arable land percentages increased from 27% in 1980, 29% in 1990, 30% in 2000, to 35% in 2010, and then decreased to 32% in 2017, fluctuating from 41.34 million km^2 in 1980 to 45.63 million km^2 in 2010. In contrast, forest area percentages decreased from 38% in 1980, 36% in 1990, 37% in 2000, to 34% in 2010, and then increased to 37% in 2017. The area percentages of grass land decreased too before 2000, ranging from 21% in 1980, 20% in 1990, and 19% in 2000, and then increased sharply thereafter, occupying around 25% in 2010-2017. Shrub land percentages occupied around 4% before 2000, and less than 0.1% thereafter. The percentages of residential area in general increased from 1% in 1980 to 2% in 2017. On the contrary, the area percentages of wetland and water body decreased from 3% and 3% in 1980 to zero and 1% in 2017, respectively. Unused lands kept unchanged through time. Since 2010, bare land has almost disappeared. Noticeably, great LULC occurred in 2000-2010 (i.e., P3 in Table 1), except for those of the wetland and bare land in 2010-2017.

3.2. Changes in soil erosion

In 1980-2017, spatial patterns of annual soil erosion rates changed little (Figure 4). Annual soil erosion rates in the NEC ranged from 0 in the plains to over 4000 t ha^{-1} yr^{-1} in the mountainous areas, with an average of 4.22 t ha^{-1} yr^{-1} (Figure 5a). It was three times the soil loss tolerance (T=1.41 t ha^{-1} yr^{-1}; [6]). Annual soil loss reached around 5.24 million ton from the NEC. The soil erosion rates were classified into five erosion classes from low (0-T), moderate (1-5T), high (5-10T), very high (10-20T) to critical (>20T). Figure 5b indicated that 57% of the NEC belonged to low erosion class, followed by moderate erosion with area covering around 30%. The high, very high and extreme erosion areas covered 6%, 3.5%, and 2.7% of the total, respectively.

Figure 4 is about here.

Figure 5 is about here.

The area percentages with different erosion classes differed with time (Figure 5). The area percentages in the low erosion class decreased from 59% in 1980 to 56% in 2010, and increased to 57% in 2017. Opposite changing patterns occurred for the area percentages with high, very high, and extreme erosion severities. The threshold values occurred in 2010. In contrast, the area percentages with moderate erosion severity increased continuously with time.

The rates of annual soil erosion presented an obvious spatial heterogeneity among the provinces and the EIM (Figure 5). The mean soil erosion rate was the highest in Liaoning Province (i.e., 9.43 t ha^{-1} yr^{-1}) in 1980-2017, followed in Jilin Province, and the EIM. The lowest erosion rate occurred in Heilongjiang Province, with an average of 2.46 t ha^{-1} yr^{-1} (Figure 5c). Considering the area percentages, their annual soil losses accounted for 21%, 17%, 26%, and 35% of the total NEC, respectively.

Temporally, the soil erosion rates of the three provinces increased from 1980 to 2010 and then decreased from 2010 to 2017. The rates of soil erosion in Heilongjiang and Jilin provinces in 2017 were less than the counterparts in 1980. The annual erosion rate in the EIM fluctuated from 1980 to 2017 (Figure 5d).

Low and moderate erosion zones dominated the area, with similar temporal patterns to the NEC (Figure 6). Specifically, the areas with low erosion class dominated Heilongjian Province, Jilin Province and the EMI, and the areas with moderate erosion class were dominant in Liaoning Province. In the three provinces, the area percentages with low erosion class decreased from 1980 to 2010, and increased from 2010 to 2017. In contrast, it continuously decreased with time in the EIM. The area percentages with moderate erosion class increased with time for Jilin Province and the EIM. In contrast, it increased in 1980-2010 and decreased from 2010 to 2017 for Heilongjiang Province, and opposite changing trend in Liaoning Province.

Figure 6 is about here.

The spatio-temporal characteristics of soil erosion severity were mapped for the 224 counties in the NEC (Figure 7). In 1980-2017, the number of the counties with soil erosion rates higher than one T accounted for around 75% of the total. The counties with soil erosion rates higher than 5T and 10T accounted for 24% and 8% of the total, respectively (Figure 8). For the top 16 counties with erosion rate higher than 10T (i.e., 14.1 t ha^{-1} yr^{-1}), 12 and 4 counties were distributed in the southeastern and southwestern NEC, respectively. Almost all the counties with soil erosion rate lower than one T were distributed in the plains (Figs. 1 and 9).

Figure 7 is about here.

Figure 8 is about here.

Arable land continuously sprawled from south to the north in1980-2010, and a little withdraw occurred in 2017. In 1980-2010, among the 224 countries, there were 52 countries in low erosion zone (i.e., less than T), 119 countries with moderate erosion zone (1-5T), 37 countries with high erosion zone (5-10T), 14 and 2 countries with very high (10-20T) and extreme erosion (> 20T) zones, respectively (Figure 8a). The number percentages of the countries with low, moderate, high, very high, and extreme zones occupied 23%, 53%, 16%, 6%, and 1% respectively.

In 1980-2017, the number percentages of the counties with low erosion rate ranged from 20% to 25% of the total and kept unchanged after 2000. The number percentages of the counties in moderate soil erosion zone decreased from 54% in 1980 to 49% in 2017, among which the soil erosion rate with 1-2T decreased fastest, from 21% in 1980 to 17% in 2017. Noticeably, the numbers of counties with high and very high classes increased from 14% and 5% in 1980 to 18% and 8%, respectively (Figure 8b).

4. Discussions

4.1. Model performance

In the NEC, soil erosion rates have been identified using runoff plot [14], ^{137}Cs tracer technique [15, 32-33], and model estimation [10, 29]. Comparisons of the RUSLE-derived rates of soil erosion in the present study to published results can evaluate the performance of the RUSLE.

Some published results are from runoff plots, natural slopes, and catchments. At plot and slope scales, the RUSLE-derived rates of soil erosion in the current study were less than the reported results (Table 3). This difference could result from two aspects. One aspect is that the 90-m resolution topographic data can smooth slope gradient [6, 34], resulting in lower soil erosion rates. The other aspect is the difference in time spans between the studies in literature and the current study. The rates of soil erosion have also been reported at larger scales, including at a 28.5 ha catchment in Heshan Farmland [15], at a 916 km^2 Shuangyang river catchment[10], and in the Sanjiang Plain [29]. A comparison at a catchment scale is more meaningful since this study was done at a large spatial scale. Table 3 demonstrated that the RUSLE-derived rates of soil erosion in the current study are basically consistent with the published results.

Table 3 is about here.

4.2. Impact of LULC change on soil erosion

Land use greatly influences soil erosion. The rates of soil erosion on bare land, shrub land, and arable land were much higher than those on other land use types, and the total soil loss amounts from these lands changed from 75% in 1980, 96% in 2010, to 79% in 2017 of the total in respect years.

Table 2 is about here.

These changes can be attributed to the LULC with time, due to population pressure and national agricultural policies [5, 11, 35]. Since the mid-20 century, extensive settlement and land exploitation have begun in the NEC, and a large amount of woodland were converted into farmland[11]. From 1980 to 2000, around 4% forest and 3% wetland were lost, and around 3381 km^2 woodland was converted to arable land in 1990-2000[12]. As a result, soil loss from arable land

accounted for 42% of the total, followed by grassland, forest land, and other land uses (Table 2). The NEC is the Chinese most important grain production base, and a series of policies further stimulated arable land reclamation in 2000-2010. For example, the rescission of the tax from agriculture in 2005 and the household responsibility system had triggered farmland cultivation at the expense of woodland (i.e., forest and shrub lands), resulting in a 46% soil loss of the total from arable land in 2010. To decrease soil loss, the "Grain to Green" project was introduced, and reforestation was initiated in the NEC [12, 36], including farmland shelterbelt, sand fixation forest, and conversion of farmland to forest on steep slopes [11]. From 2010 to 2017, forest area increased by 39,928 km^2, with the largest change ratio of 9% during 2010-2017 (Table 2).

4.3. Impact of topography on soil erosion

The spatial distribution of soil erosion rate and their changes with time can be explained by topography in the NEC. First, steep mountainous areas usually have higher LS values[36]. This distribution characteristics has been found in literatures [1, 37-38]. Second, more rainfall and higher rainfall erosivity occurred in the mountainous areas (Figure 2a), and lower values in the plains (Figure 3). The spatial pattern of R value in mountainous regions can also be found in Sudetes Mts., SW Poland[1]. In the NEC, soil erosion rates increased with increasing slope gradients (Figure 9ab). The rate of soil erosion above 300 m a.s.l. was four to five times that in areas below 200 m a.s.l. Due to steep slope and high R values, the rates of soil erosion were high in high-elevation and steep mountainous regions, and low in plains (Figure 9ab). Therefore, the spatial distributions of soil erosion rate at regional and county scales were quite related to topographic factors (Figs.1 and 5), which is consistent with the studies by Bakker et al. [39] and Latocha et al. [1]. This can explain the spatial distribution of soil erosion rate at regional and county scales in the NEC (Figures.5 and 9).

In areas with elevation above 200 m a.s.l and slopes above 5 degree, the distribution of arable land showed similar change patterns in different years, i.e., the areas of arable land increased from 1980-2010 and decreased in 2017. In contrast, in the low- elevation and gentle-slope regions, arable land area increased continuously (Figure 9cd). Because arable land is the major sediment source in the NEC and the soil erosion rate is high in the high-elevation and steep-slope areas (Table 2), the continuous sprawl of arable land in 1980-2010 and its withdrawal in 2010-2017 to the mountainous areas can explain the slightly changed distribution patterns with time (Figs.5 and 9).

Figure 9 is about here

4.4. Study limitations

The soil erosion rate was calculated through multiplying the five factors (i.e., R, K, LS, C, and P).The data accuracies, especially the values of the C and P factors, greatly influence the results. Without consideration of the varied C- and P-factor values with time could result in biased estimation [6]. Furthermore, the datasets with 90 m resolution could influence its estimation accuracy at plot or slope scales. Increase in computational capacity and high spatial resolution data could also improve estimation accuracy.

Except for data resolution, the preclusion of gully erosion from the RUSLE can also induce biased estimation. In the NEC, gullies are widely distributed, and over 295,000 (ephemeral) gullies were found in this region [40]. The soil loss from gullies is high. In a reservoir catchment in Baiquan County, the sediment from gullies occupied around 40% of the total [41]. Similar result was also obtained by Huang et al. [42] in Heshan Farmland, NEC. At a catchment scale, models like WaTEM/SEDEM [24]   and TeTIS [16] have combined soil erosion module and sediment deposition module together to simulate soil sediment yield. The combination of such module with RUSLE could improve the estimation accuracy.

The uncertainty also comes from the applications of LS calculation equations. This kind of limitation has fully been explained by Alewell et al. [43], and thus detailed explanation was not given here. However, it should be stated that the application of the upslope area-based L factor calculation could improve the estimation accuracy.

However, although such limitations and uncertainty mentioned above could to some extent influence our estimation accuracy (Table 3), the comparisons with published results verified the feasibility of our estimated results. Furthermore, since the focus of this study was to estimate the impact of LULC on soil erosion with time, these uncertainties can be accepted.

5. Conclusions

Assessment of the impact of regional LULC change on soil loss is paramount importance to appropriately regulate land use. Soil loss characteristics and its changing patterns following LULC changes in 1980-2017 were explored using RUSLE method at regional, provincial, and county scales.

In the NEC, higher rates of soil erosion occurred in the mountainous regions, and lower values in the plains. The spatial patterns of soil loss coincided with those of RUSLE-LS, -C, -K, and -R factors in the NEC (Figs. 2 and 4). Impacted by the LULC in 1980-2017, threshold values of soil erosion rate occurred. The regional soil erosion rates increased from 3.91 t ha^{-1} yr^{-1} in 1980 to 4.45 t ha^{-1} yr^{-1} in 2010 and decreased to 4.22 t ha^{-1} yr^{-1} in 2017. The rates of soil erosion less than the tolerance value (i.e., 1.41 t ha^{-1} yr^{-1}) decreased from 1980 to 2010, and increased in 2017. In contrast, opposite changing patterns occurred in higher erosion classes. At provincial scale, due to higher R values in the southeast and southwest of the NEC, the highest soil erosion rate of 9.43 t ha^{-1} yr^{-1} occurred in Liaoning Province, and the lowest value in Heilongjing Province. Due to the sprawl of arable lands at the expense of natural vegetation from 1980 to 2010, the area percentages with soil erosion rate higher than 7.05 t ha^{-1} yr^{-1} increased before 2010, and decreased after 2010. At a county scale, the counties in the southeast and southwest of the NEC experienced the highest soil loss. Around 75% of the counties suffered soil loss with soil erosion rate higher than its tolerance level. The areas with soil erosion rate less than T increased in 1980-2010 and decreased in 2017. Therefore, appropriate policies can control soil loss through limiting the sprawl of arable lands in unfavorable regions.

Author contributions: Haiyan Fang collected information and wrote the paper. Zemeng Fan contributed to statistical analysis and revised the manuscript.

Competing interests: The authors declare no competing interests.

References

1. Latocha, A.; Szymanowski, M.; Jeziorska, J.; Stec, M.; Roszczewska, M. Effects of land abandonment and climate change on soil erosion-An example from depopulated agricultural lands in the Sudetes Mts., SW Poland. *Catena* **2016,***145*, 128-141.

2. Cerdan, O.; Gover, G; Le Bissonnais, Y.; Van Oost, K.; Posen, J.; Saby, N.; Gobin, A.; Vacca, A.; Quinton, J.; Auerswald, K.; Klik, A.; Kwaad, F.J.P.M.; Raclot, D.; Rejman, J.; Rousseva, S.; Muxart, T.; Roxo, M.J.; Dostal, T. Rates and spatial variations of soil erosion in Europe: a study based on erosion plot data. *Geomorphology* **2010,** *122 (1-2)*, 167-177.

3. Anh, P.T.O.; Gomi, T.; Macdonald, L.H.; Mizugaki, S.; Van Khoa, P.; Furuichi, T. Linkages among land use, macronutrient levels, and soil erosion in northern Vietnam: A plot-scale study. *Geoderma* **2014**, 232-234, 352-362.

4.   Anache, J. A.; Wendland, E. C., Oliveira, P. T.; Flanagan, D. C.; Nearing, M. A. Runoff and soil erosion plot-scale studies under natural rainfall: A meta-analysis of the Brazilian experience. *Catena* **2017**, *152*, 29-39.

5.   Zare, M.; Panagopoulos, M.; Loures, L. Simulating the impacts of future land use change on soil erosion in the Kasilian watershed, Iran. *Land Use Pol.* **2017**, *67*, 558-572.

6.   Duan, X.W.; Bai, Z.W.; Rong, L.; Li, Y.B.; Ding, J.H.; Tao, Y.Q.; Li, J.X.; Li, J.H.; Wang, W. Investigation method for regional soil erosion based on the Chinese Soil Loss Equation and high-resolution spatial data: Case study on the mountainous Yunnan Province, China. *Catena* **2020**, *184*, 104237.

7.   Borrelli, P.; Van Oost, K.; Meusburger, K.; Alewell, C.; Lugato, E.; Panagos, P. An assessment of the global impact of 21st century land use change on soil erosion. *Nat. Commun.* **2017**, *8*, 2013.

8.   Siswanto, S.Y.; Francés, F. How land use/land cover changes can affect water, flooding and sedimentation in a tropical watershed: a case study using distributed modeling in the Upper Citarum watershed, Indonesia. *Environ. Earth Sci.* **2019,** *78*, 550.

9.   Xie, Y.; Liu, H.H.; Ye, Y.; Ren, X.Y. Changes in soil erosion in cropland in northeastern China over the past 300 years. *Catena* **2019**, *176*, 410-418.

10. Fang, H.Y.;   Sun, L.Y. Modelling soil erosion and its response to the soil conservation measures in the black soil catchment, Northeastern China. *Soil Tillage Res.* **2017,** *165*, 23-33.

11. Xu, X.Z.; Xu, Y.; Chen, S.C.; Zhang, H.W. Soil loss and conservation in the black soil region of Northeast China: a retrospective study. *Environ. Sci. Pol.* **2010**, *13*, 793-800.

12. Mao, D.H.; He, X.Y.; Wang, Z.M.; Tian, Y.L.; Xiang, H.X.; Yu, H.; Man, W.D.; Jia, M.M.; Ren, C.Y.;   Zheng, H.F. Diverse policies leading to contrasting impacts on land cover and ecosystem services in Northeast China. *J. Clean. Prod.* **2019**, *240*, 117961.

13. Zhang, X.K., Xu, J.H., Lu, X.Q., Deng, Y.J., & Gao, D.W. A study on the Soil Loss Equation in Heilongjiang Province. *Soil Water Conserv. 12 (4)*, 1-9, 18 (1992).

14. Liu, B.; Yan, B.; Shen, B.; Wang, Z.; Wei, X. Current status and comprehensive control strategies of soil erosion for cultivated land in the Northeastern black soil area of China. *Sci. Soil and Water Conserv.* **2018**, *6*, 1-8.

15. Fang, H.Y.; Sun, L.Y.; Qi, D.L.; Cai, Q.G. Using ^{137}Cs technique to quantify soil erosion and deposition rates in an agricultural catchment in the typical black soil region, Northeast China. *Geomorphology* **2012**,

169-170, 142-150.

16.   Li, Z.Y.; Fang, H.Y. Modeling the impact of climate change on watershed discharge and sediment yield in the black soil region, northeastern China. *Geomorphology* **2017**, *293,* 255-271.

17.   Ouyang, W.; Wu, Y.Y.; Hao, Z.C.; Zhang, Q.; Bu, Q.W.; Gao, X. Combined impacts of land use and soil property changes on soil erosion in a mollisol area under long-term agricultural development. *Sci. Tot. Environ.* **2018**, *613-614,* 798-809.

18.   Fang, H.Y. Impact of land use change and dam construction on soil erosion and sediment yield in the black soil region, northeastern China. *Land Degrad. Dev.* **2017**, *28,* 1482-1492.

19.   Jiang, C., Zhang, L., & Zhang, H. Quantitative evaluation of soil conservation in 2000-2010 in Heilongjiang Province using RUSLE model. *Chin. J. Eco-Agric.* **2015**, *23 (5),* 642-649.

20.   Sun, J.M.; Liu, T.S. Desertification in the Northeastern China. *Qu. Sci.* **2001**, *21,* 72-78.

21.   Wischmeier, W.H.; Smith, D.D. Predicting Rainfall Erosion Losses: A Guide to Conservation Planning. Agriculture Handbook Number 537. United States Department of Agriculture, **1978**.

22.   Lee, J.K.; Heo, J.H. Evaluation of estimation methods for rainfall erosivity based on annual precipitation in Korea. *J. Hydrol.* **2011**, *409,* 30-48.

23.   Zhang, W.B.; Fu, J.S. Using different types of rainfall datasets to estimate rainfall erosivity. *Res. Sci.* **2003**, *25(1),* 26-28.

24.   Van Rompaey, A.J.J.; Verstraeten, G.; Van Oost, K.; Govers, G.; Poesen, J. Modelling mean annual sediment yield using a distributed approach. *Earth Surf. Processes Landforms* **2001**, *26,* 1221-1236.

25.   McCool, D.K.; Foster, G.R.; Mutchler, C.; Meyer, L. Revised slope length factor for the universal soil loss equation. *Trans. ASAE* **1989**, *32,* 1571-1576.

26.   Desmet, P.; Govers, G. A GIS procedure for automatically calculating the USLE LS factor on topographically complex landscape units. *J. Soil Water Conserv.* **199**6, *51,* 427-433.

27.   Renard, K.G.; Foster, G.R.; Weesies, G.A.; McCool, D.K.; Yoder, D.C. Predicting Soil Erosion by Water: A Guide to Conservation Planning with the Revised Universal Soil Loss Equation (RUSLE). Agriculture Handbook Number 703. United States Department of Agriculture, **1997**.

28.   Wei, J.B.; Xiao, D.N.; Li, X.Z.; Bu, R.C.; Zhang, C.S. Relationship between landscape pattern and soil erosion of an agricultural catchment in the Mollisols region of northeastern China. *Acta Ecol. Sin.* **2016**, *26 (8),* **2608**-2615.

29.   Zhang, S.W.; Wang, W.J.; Li, Y.; Bu, K.; Yan, Y.C. Dynamics of hillslope soil erosion in the Sanjiang plain in the past 50 years. *Resour. Sci.* **2008**, *30 (6)*, 843-849.

30.   Wang, W.J.; Zhang, S.W.; Fang, H.Y. Couple relationships between slope and gully erosions in the typical black soil regions, Northeastern China. *J. Nat. Resour.* **2012**, *27*, 2113-2122.

31.   Sheng, M.; Fang, H.Y.; Sun, Y.R.; Guo, M. Analysis of the factors influencing catchment sediment yield for the black soil region. *J. Shaanxi Nor. Uni. (Nat. Sci. Edi.)* **2015**, *43*, 86-92.

32.   Wei, X. Study on the Spatial Variations of Soil Erosion in Drainage Basin of the Black Soil Region of Northeast China. Beijing Normal University, Beijing, China **2007.**

33.   Yu, H.Q.; Li, Y.; Nguyen, M.L.; Funk, R.; Liu, Q.G.; Li, J.J. Fallout radionuclide based techniques for assessing the effectiveness of soil conservation measures in different eroded regions of China. *J. Nucl. Agric. Sci.* **2012**, *26 (2)*, 340-347.

34.   Chang, K.; Tsai, B. The effect of DEM resolution on slope and aspect mapping. *Inform. Syst.* **1991**, *18 (1)*, 69-77.

35.   Devátý, J.; Dostál, T.; Hösl, R., Krása, J.; Strauss, P. Effects of historical land use and land pattern changes on soil erosion - Case studies from Lower Austria and Central Bohemia. *Land Use Pol.* **2019,** *82*, 674-685.

36.   Gao, J.; Liu, Y.S.; Chen, Y.F. Land cover changes during agrarian restructuring in Northeast China. *Appl. Geogr.* **2006**, *26*, 312-322.

37.   Vijith, H.; Hurmain, A.; Dodge-Wan, D. Impacts of land use changes and land cover alteration on soil erosion rates and vulnerability of tropical mountain ranges in Borneo. *Remote Sens. Appl. Soc. Environ.***2018**, *12*, 57-69.

38.   Teng, H.F.; Liang, Z.Z.; Chen, S.C.; Liu, Y.; Viscarra Rossel, R.A.; Chappell, A.; Yu, W.; Shi, Z. Current and future assessments of soil erosion by water on the Tibetan Plateau based on RUSLE and CMIP5 climate models. *Sci.Tot. Environ.* **2018**, *635*, 673-686.

39.   Bakker, M.M.; Govers, G.; van Doorn, A.; Quetier, F.; Chouvardas, D.; Rounsevell, M. The response of soil erosion and sediment export to land-use change in four areas of Europe: the importance of landscape pattern. *Geomorphology* **2008**, *98*, 213-226.

40.   Dong ,Y.F.; Wu, Y.Q.; Qin, W.; Guo, Q.K.; Yin, Z.; Duang, X.W. The gully erosion rates in the black soil region of northeastern China: Induced by different processes and indicated by different indexes. *Catena* **2019**, *182*, 104146.

41.   Fang, H.Y. Temporal variations of sediment source from a reservoir catchment in the black soil region,

Northeast China. *Soil Tillage. Res.* **2015**, *153*, 59-65.

42.   Huang, D.H.; Du, P.F.; Wang, J.; Wei, X.; Liu, B.; Xu, J.J. Using reservoir deposits to quantify the source

contributions to the sediment yield in the Black Soil Region, Northeast China, based on the fingerprinting

technique. *Geomorphology* **2019**, *339*, 1-18.

43.   Alewell, C.; Borrelli, P.; Meusburger, K.; Panagos, P. Using the USLE: Chances, challenges and limitations

of soil erosion modeling. *Int. Soil Water Conserv. Res.* **2019,** *7*, 203-225.

Table 1. Area percentage of each landuse class in 1980-2017 and their change rates ($R=100*(Area_{i+1}-Area_i)/Area_i$; i recurrents the year used) in different time phases P1 (1980-1990), P2(1990-2000), P3 (2000-2010), and P4 (2010-2017).

	%1980	%1990	%2000	%2010	%2017	%P1	%P2	%P3	%P4
Arable land	27	29	30	35	32	7	3	**16**	-7
Forest	38	37	37	34	37	-4	0	-7	**9**
Grassland	21	20	19	25	25	-4	-2	**30**	-3
Shrub land	3	4	4	0	0	20	-9	**-98**	67
wetland	4	4	3	1	0	-5	-5	-66	**-98**
Water body	3	3	2	1	1	-1	-4	**-50**	0.00
Residential areas	2	2	2	2	2	4	-1	-1	**6**
Bare land	1	1	1	1	2	3	-11	36	**80**
Other unused lands	1	1	1	0	0	-19	24	**-100**	0

Note: the bold value indicates the largest change rate for each LULC classes in the row. Positive values indicate more land area occurred in the second year, and negative values indicate more lands in the first year.

Table 2. The mean soil erosion rate (t ha^{-1} yr^{-1}), soil loss amount (SLA; 10^6 t), and their percentage (%) of the total as well as their mean values of the five years for each land use class.

LULC class	1980			1990			2000		
	Mean	SLA	Percent	Mean	SLA	Percent	Mean	SLA	Percent
Arable	5.59	199.82	40	6.07	216.95	40	5.80	214.12	42
Forest	1.74	79.11	16	1.73	78.82	14	1.77	80.56	16
Grassland	4.05	99.74	20	4.30	105.86	20	4.34	104.28	20
Shrubland	15.83	79.05	16	18.37	91.70	17	15.27	69.33	13
Water area	0.00	0.00	0	0.00	0.00	0	0.00	0.00	0
Unused land	0.85	1.15	0	0.42	0.57	0	0.38	0.64	0
Residential	1.45	4.25	1	1.49	4.35	1	1.45	4.20	1
Bare land	34.49	42.19	8	39.03	47.74	9	37.95	41.50	8
	2010			2017			Five-year mean		
	Mean	SLA	Percent	Mean	SLA	Percent	Mean	SLA	Percent
Arable	5.98	256.52	46	4.47	178.53	34	5.58	213.19	40
Forest	1.76	74.57	14	1.77	82.13	16	1.75	79.04	15
Grassland	6.32	197.97	36	4.92	149.61	29	4.79	131.49	25
Shrubland	6.59	0.53	0	58.35	7.06	1	22.88	49.53	9
Water area	0.00	0.00	0	0.00	0.00	0	0.00	0.00	0
Unusedland	9.58	0.01	0	8.71	0.00	0	3.99	0.47	0
Residential	1.31	3.76	1	1.88	5.72	1	1.52	4.46	1
Bareland	12.54	18.60	3	36.08	96.69	19	32.02	49.34	9

Table 3. The published rates of soil erosion in the black soil region (the study area locations of the references are labeled in Figure 1).

Region	Time	Gradient (°)	Land use	Size	Method	Erosion rate ($mm\ yr^{-1}$)	Erosion rate* ($t\ ha^{-1}\ yr^{-1}$)	Current study	Reference
1-1	2005	3-5	UPC	Natural slope	^{137}Cs tracer	3.90	50.7	15.76	Liu et al., 2008
1-2	2005	2.2-3.5	UPC	Natural slope	^{137}Cs tracer	1.87	24.31	12.81	Liu et al., 2008
3-1	2003-2004	6-10	UPC	Natural slope	^{137}Cs tracer	-	29.0	20.0	Yu et al., 2012
5-1	2004	2.8	UPC	Natural slope	^{137}Cs tracer	1.80	23.40	6.1	Liu et al., 2008
5-2	2005	0.5-3.5	UPC	Natural slope	^{137}Cs tracer	1.00-2.66	21.76	11.4	Liu et al., 2008
4-1	1985-1990	5.0	Bare land	20-m plot	Monitoring	1.97	25.61	18.7	Liu et al., 2008
2	1985-1990	5.0	Bare land	20-m plot	Monitoring	3.31	43.03	16.4	Liu et al., 2008
5-1	2003-2004	5.0	Bare land	20-m plot	Monitoring	3.91	50.83	16.4	Liu et al., 2008
5-2	2003-2004	1.6	UPC	100-m plot	Monitoring	0.65	8.45	1.43	Liu et al., 2008
5-3	2003-2004	2.0	UPC	200-m plot	Monitoring	0.89	11.57	2.5	Liu et al., 2008
3-2	1980-1985	5	UPC	20-m plot	Monitoring	0.456	6.84	4.35	CGWCR
3-3	1980-1985	5	UPC	20-m plot	Monitoring	0.198	2.97	4.35	CGWCR
5-4	2011	0-3	UPC	28.5 ha catchment	^{137}Cs tracer	-	2.2	2.8	Fang et al., 2012
5-5	2007	0-5	UPC	3 km^2 catchment	^{137}Cs tracer	-	11.10	2.67	Wei, 2007
3-4	2010	0-8	Forest	916 km^2 catchment	Modelling	-	1.48	1.77	Fang and Sun, 2017
3-5	2010	0-8	Shrub land	916 km^2 catchment	Modelling	-	2.58	5.27	Fang and Sun, 2017
3-6	2010	0-8.16	Grass land	916 km^2 catchment	Modelling	-	1.09	4.33	Fang and Sun, 2017
3-7	2010	0-8.16	Multiple	916 km^2 catchment	Modeling	-	2.58	2.54	Fang and Sun, 2017
6	2002	0-40	Multiple	108,900 km^2	Modelling		2.26	1.81	Zhang et al., 2008

Note: * The average bulk density 1.3 t m^{-3} was used when the unit mm yr^{-1} was converted to unit t ha^{-1} yr^{-1} according to Xie et al. (2019); CGWCR indicates the Complication Group of Water Conservancy Record in Baiquan County; UP recurrents up-down cultivated land. The first numbers in the column "Region" recurrent the counties labeled in Figure 1.

Figure captions:

Figure 1. Study area map showing the location, topography, meteorological station, the validation site in the current study (a), slope gradient distribution (b), precipitation in 1970-2018 (c), and soil types (d). The numbers in Figure 1a indicate the site of the published papers used for verifying our results in the current study (1 Dehui County; 2 Binxian County; 3 Baiquan County; 4 Keshan County; 5 Heshan Farmland; 6 Sanjiang Plain).

Figure 2. The RUSLE input maps of the (a) LS factor, (b) R factor, and (c) K factor.

Figure 3. Land use maps in 1980, 1990, 2000, 2010, and 2017 for the NEC.

Figure 4. The spatial distribution characteristics of the soil erosion rates in 1980, 1990, 2000, 2010, 2017, and their average in 1980-2017.

Figure 5.Changes of the mean annual erosion rate (a) and different erosion classes (b) in the whole NEC with time, and soil erosion rates for three provinces and the ETM (c) as well as their changes with time (d). (The soil loss tolerance T = 1.14 t ha^{-1} yr^{-1})

Figure 6. Area percentages of different erosion grades in Heilongjiang Province (a), Jilin Province (b), Liaoning Province (c), and (d) the IMA.

Figure 7. Maps showing the mean rate of soil erosion in 1980, 1990, 2000, 2010, 2017, and the average during the study period at a county scale in the NEC.

Figure 8. Changes of the number of counties (a) and the number percentages (b) with different soil erosion grades during 1980-2017.

Figure 9. Distribution characteristics of soil erosion rates and the arable land areas according to altitude (a,c), and slope gradient (b,d) in the years 1980, 1990, 2000, 2010, and 2017.
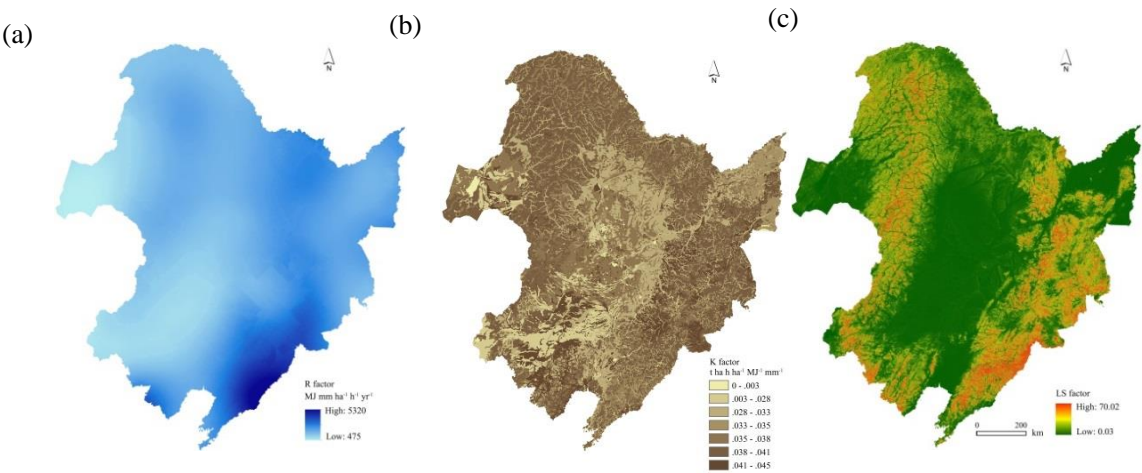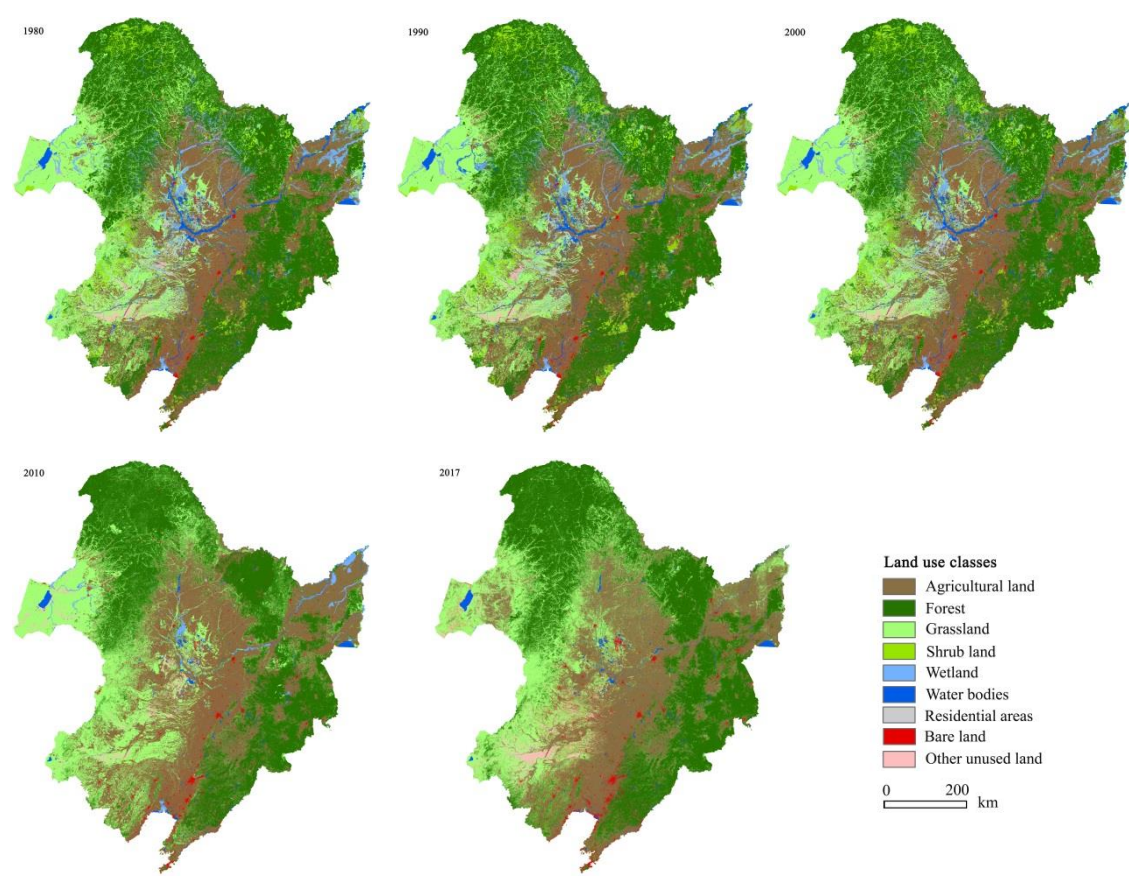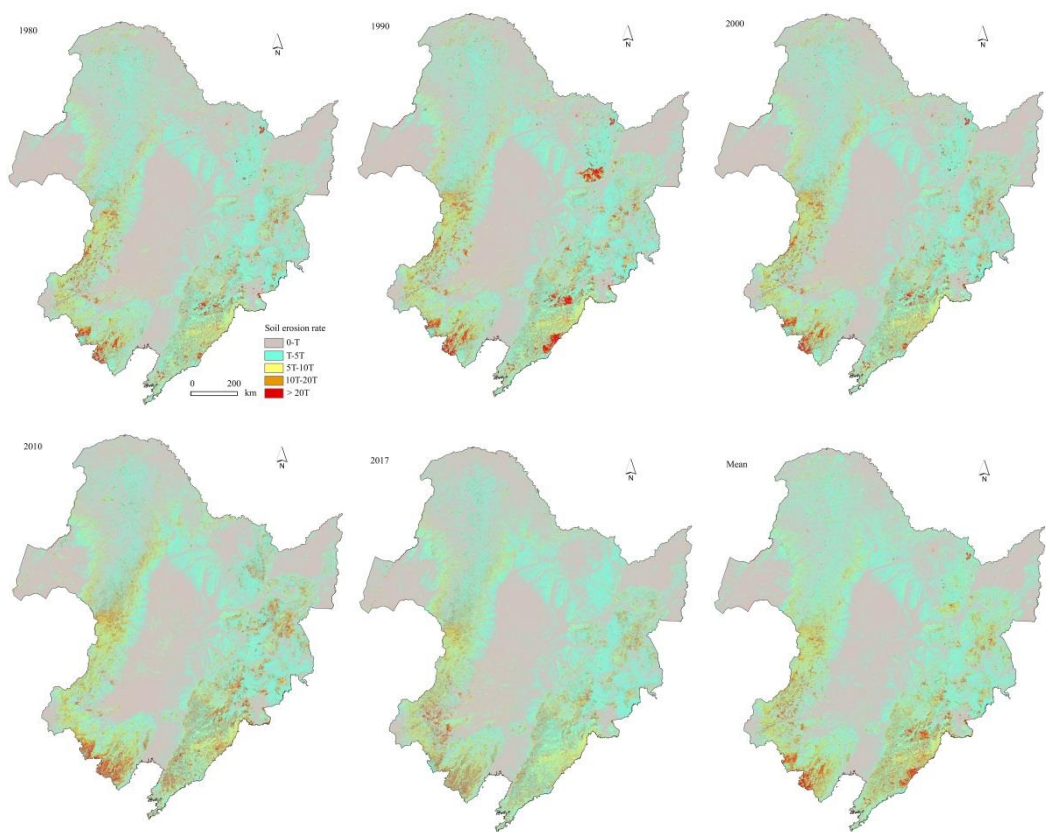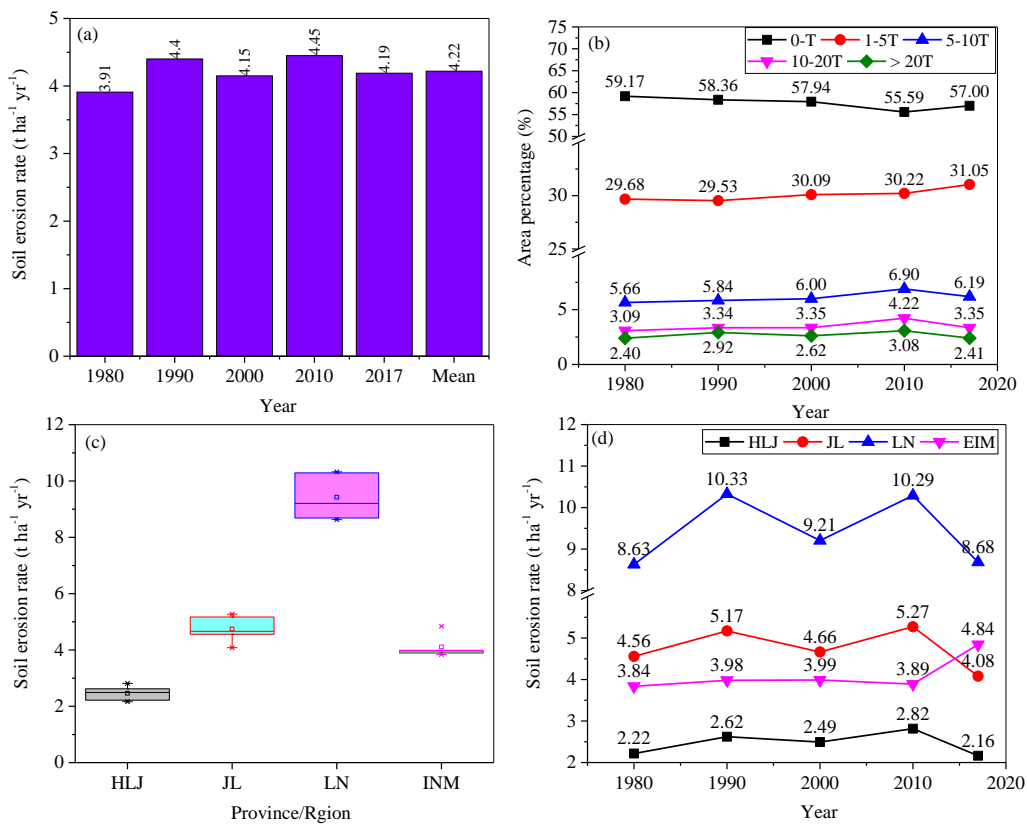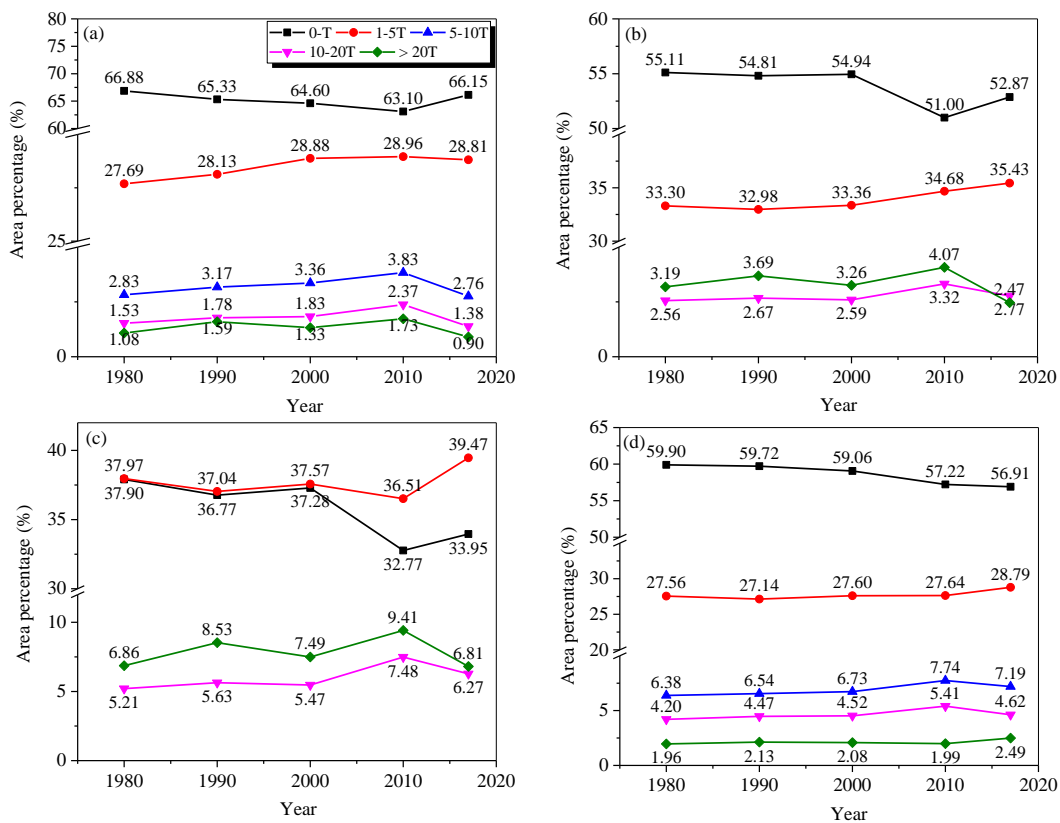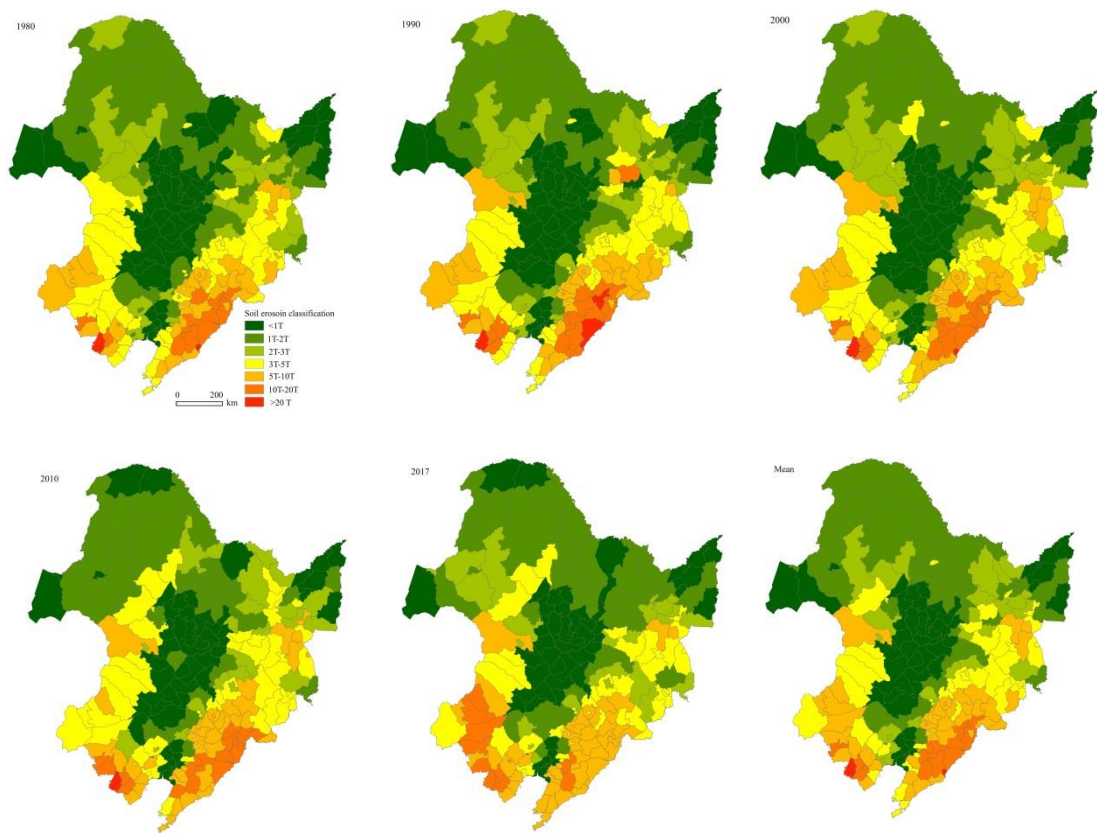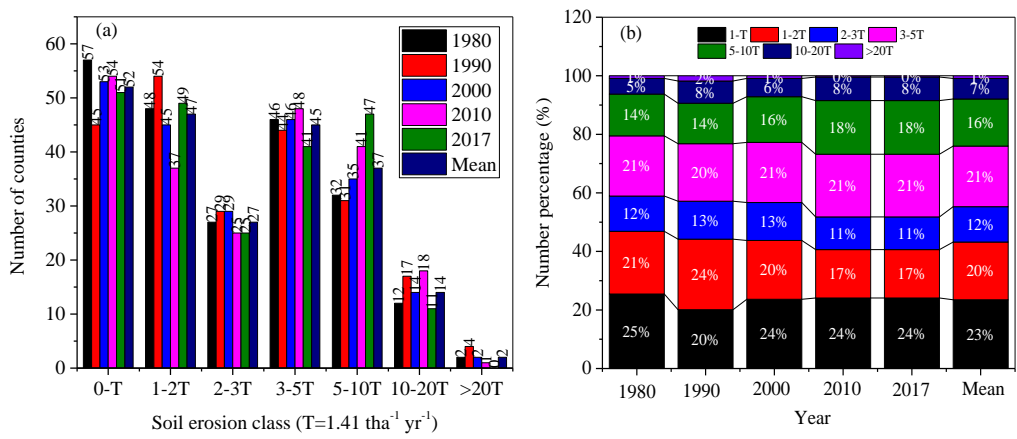
Figure 1.
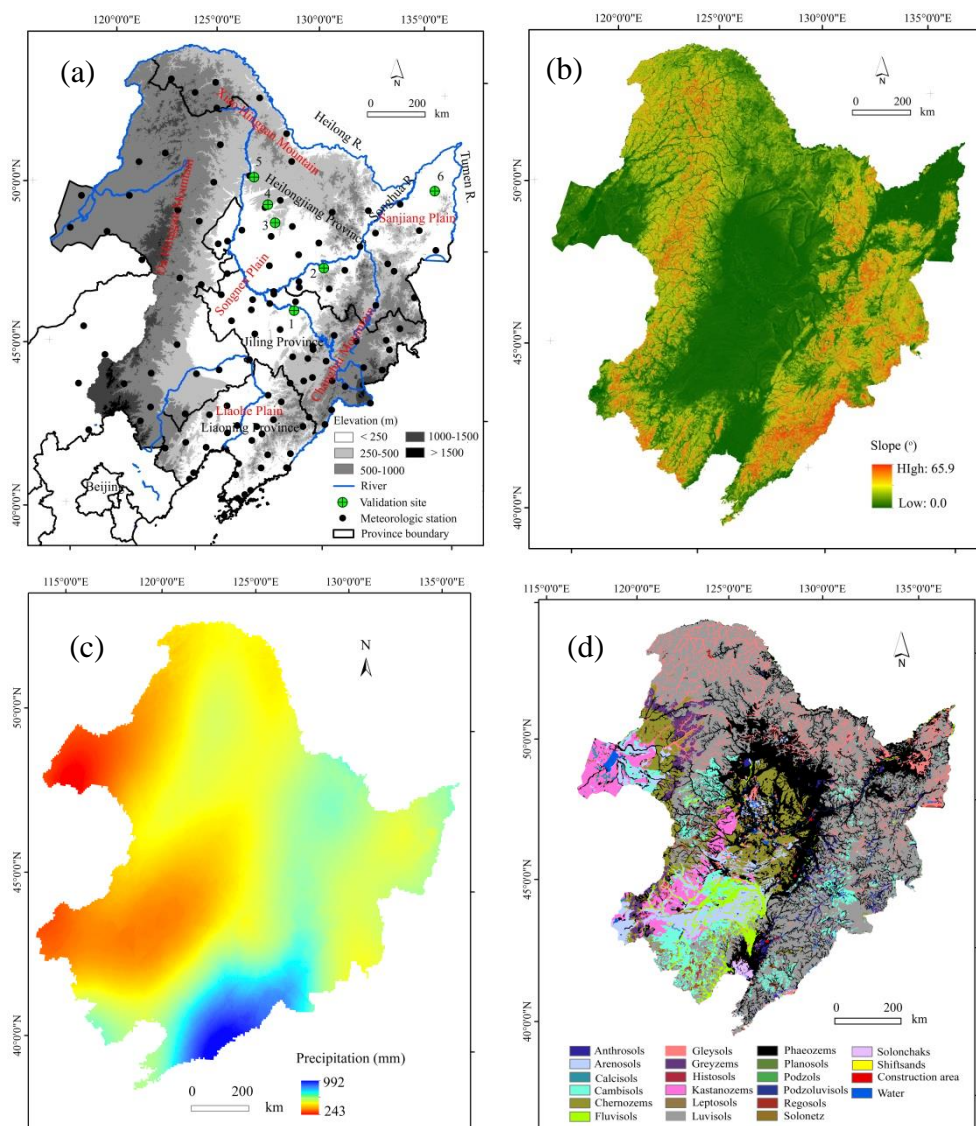
Figure 2.

Figure 3.

Figure 4.

Figure 5.

Figure 6.

Figure 7.

Figure 8.

Figure 9.